Since January 2020 Elsevier has created a COVID-19 resource centre with free information in English and Mandarin on the novel coronavirus COVID-19. The COVID-19 resource centre is hosted on Elsevier Connect, the company's public news and information website.

Journal of Molecular Structure 1271 (2023) 133992

Contents lists available at ScienceDirect

Journal of Molecular Structure

journal homepage: www.elsevier.com/locate/molstr

Synthesis and characterization of two known and one new impurities of dolutegravir: *In silico* evaluation of certain intermediates against SARS CoV-2 O-ribose methyltransferase (OMTase)

Sailaja Garrepalli[a,b], Ramesh Gudipati[b], Ravikumar Kapavarapu[c], Kunta Ravindhranath[a,*], Manojit Pal[d,*]

[a] Department of Chemistry, Koneru Lakshmaiah Education Foundation, Guntur District, Vaddeswaram, Andhra Pradesh 522502, India
[b] Synix Labs, 5-5-35/33/1, NCS complex, First floor, Prashanth nagar, Kukatpally, Hyderabad, Telangana 500072, India
[c] Nirmala College of Pharmacy, Mangalagiri, Andhra Pradesh, India
[d] Dr. Reddy's Institute of Life Sciences, University of Hyderabad Campus, Hyderabad 500046, India

ARTICLE INFO

Article history:
Received 9 February 2022
Revised 20 July 2022
Accepted 19 August 2022
Available online 20 August 2022

Keywords:
Dolutegravir
Impurities
Synthesis
In silico study

ABSTRACT

Besides its use against HIV infection the marketed anti-retroviral drug dolutegravir attracted attention as a potential agent against COVID-19 in multiple AI (artificial intelligence) based studies. Due to our interest in accessing the impurities of this drug we report the synthesis and characterization of three impurities of dolutegravir one of which is new. The synthesis of O-methyl ent-dolutegravir was accomplished in three-steps the first one involved the construction of fused 1,3-oxazinane ring. The cleavage of –OEt ether moiety followed by methylation afforded the target compound. The second impurity i.e. *N*-(2,4-difluorobenzyl)-4-methoxy-3-oxobutanamide was synthesized *via* a multi-step method involving sequentially the keto group protection, ester hydrolysis, acid chloride formation followed by the reaction with amine and finally keto group deprotection. The synthesis of new or dimer impurity was carried out *via* another multi-step method similar to the previous one starting from ethyl 4-chloro acetoacetate. The methodology involved preparation of ether derivative, keto group protection, ester hydrolysis, preparation of amide derivative *via* acid chloride formation *in situ* and then keto group deprotection for a longer duration. The last step afforded the target compound for which a plausible reaction mechanism has been proposed. All three impurities were prepared in gram scale (minimum 2 g and maximum 8 g). The *in silico* evaluation of three selected synthesized intermediates e.g. **7, 8** and **9** (structurally similar to dolutegravir) against SARS CoV-2 O-ribose methyltransferase (OMTase) (PDB: 3R24) indicated that compound **7** could be of interest as a possible inhibitor of this protein.

1. Introduction

With over 37 million people currently being affected worldwide [1–3] by HIV, the disease remained as one of the major health concerns. While a range of treatments have been introduced to control this disease [4,5] however the high cost often poses an economic burden for patients especially in countries belonging to lower-income group. Launched in the market in 2013 under the umbrella of second generation integrase inhibitors [6] the anti-HIV drug dolutegravir (GSK1349572; brand name 'Tivicay') was developed by GlaxoSmithKline (GSK) and Shionogi. The mechanism of action (MOA) of dolutegravir involves inhibition of the HIV integrase *via* binding to the integrase active site that in turn blocks the strand transfer and integration of retroviral deoxyribonucleic acid (DNA). As a result, the HIV replication cycle is blocked [7]. Indeed, dolutegravir has shown remarkably potent antiviral activity along with high genetic barrier to resistance and the drug is currently in use for treating a broad population of HIV-infected patients. Apart from being used as an anti-retroviral drug dolutegravir was also listed along with several other molecules such as atazanavir, efavirenz, ritonavir, raltegravir, bictegravir as possible agents against SARS-CoV-2 (severe acute respiratory syndrome coronavirus-2) in multiple artificial intelligence (AI) based studies. Indeed, dolutegravir was predicted to interact with nCoV 2′-

Abbreviations: OMTase, SARS CoV-2 O-ribose methyltransferase; SARS-CoV-2, severe acute respiratory syndrome coronavirus-2.

* Corresponding authors.
E-mail addresses: ravindhranath.kunta@gmail.com (K. Ravindhranath), manojitpal@rediffmail.com (M. Pal).

https://doi.org/10.1016/j.molstruc.2022.133992
0022-2860/

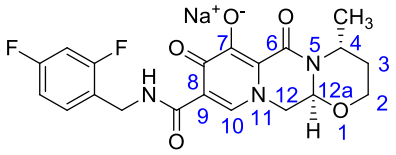

Fig. 1. Chemical structure of marketed drug dolutegravir sodium.

OMTase (2′-O-ribose methyltransferase) that methylates the ribose 2′-O position of the first and second nucleotide of viral mRNA for evading the host immune system [8–10]. While these observations required further validations *in vitro* and *in vivo* the already marketed dolutegravir showed considerable potential to be repurposed against COVID-19, a pandemic that resulted in a record number of infected people worldwide.

Chemically, dolutegravir (Fig. 1) contains a hexahydro-2*H*-pyrido[1′,2′:4,5]pyrazino[2,1-*b*][1,3]oxazine framework that is connected to the 2,4-difluorobenzene ring *via* an amide based linker i.e. -CONHCH$_2$-. The compound has two carbonyl groups at C-6 and C-8 position and an enolic hydroxy group at C-7 of the fused heterocyclic moiety. The compound is a (4R,12aS) enantiomer. The initial synthesis of dolutegravir was reported in 2006 [11] and a new process for the preparation of dolutegravir was disclosed in 2015 [12] (Scheme 1). The compound **1** prepared from ethyl-4-chloroacetoacetate *via* several steps was used as a key intermediate in this process. As part of the process research a number of impurities related to this drug were identified and disclosed [13,14]. Efforts on the respective chemical synthesis and subsequent spectral characterization [13–15] helped in confirming the structure of some of these potential impurities. Notably, the identification, isolation and characterization of impurities related to a particular API (active pharmaceutical ingredient) product are considered as essential activities for obtaining the required approvals from the regulatory agency (RA) [16,17]. Previously we have reported synthesis and characterization of certain impurities of dolutegravir [15]. In further continuation of this work we now report synthesis and spectroscopic characterization (e.g. IR, ^{1}H & ^{13}C NMR, Mass, HRMS and HPLC) of some other impurities related to this drug e.g. O-methyl ent-dolutegravir (or compound **9**), *N*-(2,4-difluorobenzyl)-4-methoxy-3-oxobutanamide (or compound **14**) and a dimer impurity (or compound **19**) (Fig. 2). Notably, the dimer impurity **19** appeared to be a new compound and was detected during our effort on process development of dolutegravir. Particularly, the use of intermediate i.e. *N*-(2,4-difluorobenzyl)-2-(2-(methoxymethyl)-1,3-dioxolan-2-yl)acetamide for the preparation of compound **1** of Scheme 1 afforded the impurity **19** as a side product. Nevertheless, the results of *in silico* evaluation of some of these impurities against COVID-19 are also presented.

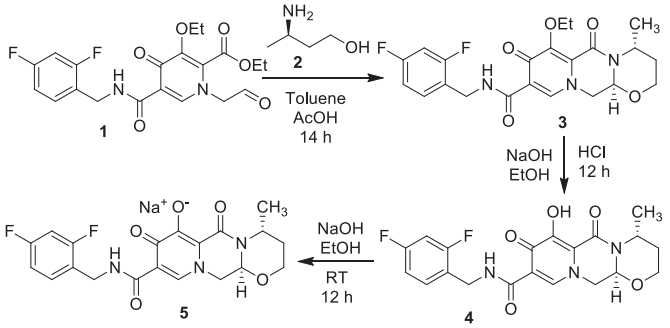

Scheme 1. Reported process for dolutegravir starting from intermediate **1** [12].

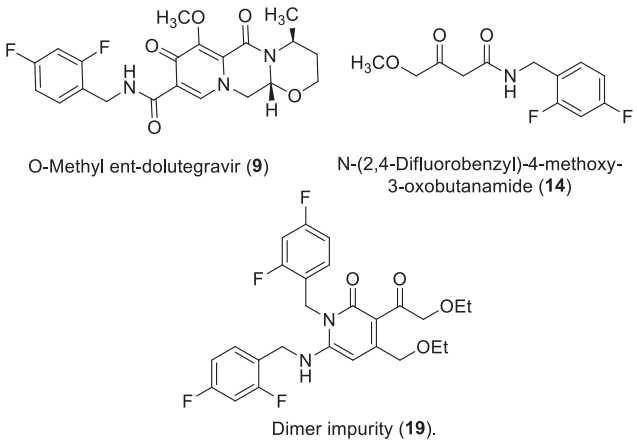

Fig. 2. Chemical structure of three impurities of dolutegravir.

2. Results and discussion

The synthesis of O-methyl ent-dolutegravir or compound **9** is depicted in Scheme 2. The intermediate i.e. ethyl 5-((2,4-difluorobenzyl)carbamoyl)-3-ethoxy-4-oxo-1-(2-oxoethyl)-1,4-dihydropyridine-2-carboxylate (**1**) used previously in the process development (Scheme 1) was also used as the staring compound in the current synthesis. The reaction of this polyfunctionalized substrate **1** with (*S*)-3-amino-1-butanol (**6**) in toluene in the presence of acetic acid furnished the hemiaminal ether derivative **7** in good yield. The reaction proceeded *via* participation of the aldehyde moiety of substrate **1** and the amino as well as hydroxy group of the reactant **6** to form the 1,3-oxazinane ring of product **7**. This was further indicated by the ^{1}HNMR spectra [where the newly introduced C-4 methyl group appeared at δ 1.35 (d, J = 7.2 Hz, 3H)] along with MS [*m/z*: 448 (M+H)$^+$] recorded for product **7**. Treating this ethyl ether derivative **7** with NaOH in EtOH at room temp followed by usual acid work-up afforded the desired product **8** (in 70% yield with the HPLC purity of 99.03%) the spectral data of which was recorded and compared with dolutegravir for further confirmation. The omission of proton signals at δ 1.47 (t, J = 7.0 Hz, 3H, CH$_3$) and 3.96 (m, 2H, OCH$_2$) in the ^{1}HNMR spectra of **8** indicated the removal of ethyl group from OEt moiety of **7**. On treatment with dimethyl sulfate in the presence of K_2CO_3 in acetone the compound **8** furnished the O-methyl ent-dolutegravir (**9**) in 80% yield (with the HPLC purity of 95.66%). Besides MS [*m/z*: 434 (M+H)$^+$] and HRMS [calcd for $C_{21}H_{21}F_2N_3O_5$ (M+H)$^+$ 434.1483, found 434.1481] the compound **9** was characterized by the NMR and IR spectra. The IR absorption

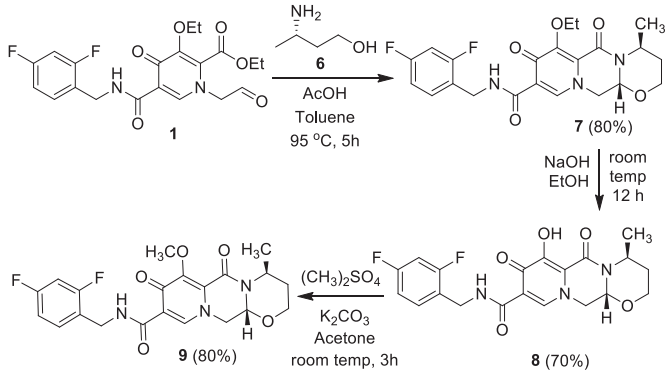

Scheme 2. Synthesis of O-methyl ent-dolutegravir or compound **9** from (*S*)-3-amino-1-butanol.

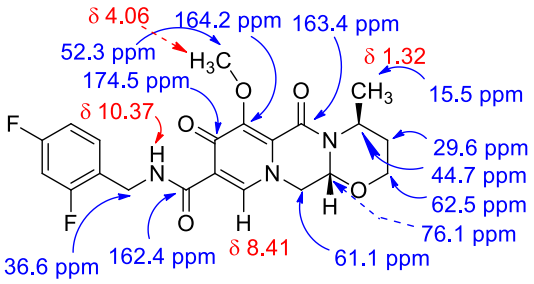

Fig. 3. Presentation of partial ^{1}H (red) and ^{13}C NMR data (blue) of compound **9**.

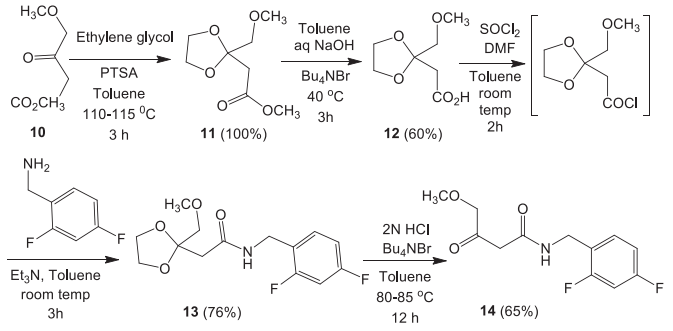

Scheme 3. Synthesis of *N*-(2,4-difluorobenzyl)-4-methoxy-3-oxobutanamide or compound **14** *via* a multi-step method.

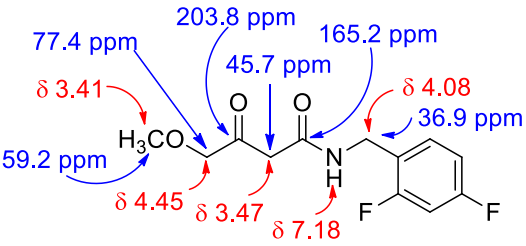

Fig. 4. Presentation of partial ^{1}H (red) and ^{13}C NMR data (blue) of compound **14**.

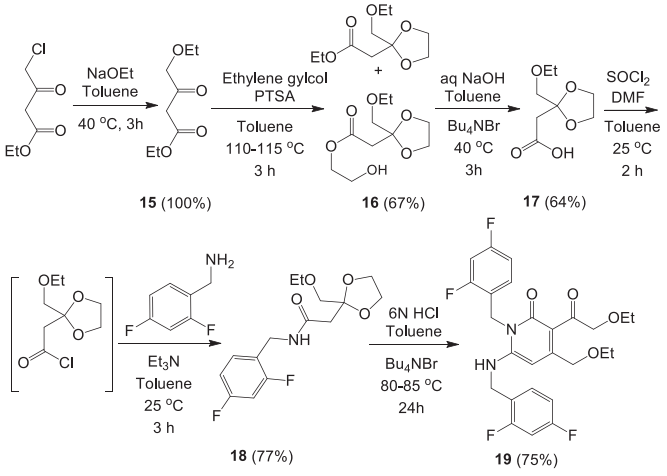

Scheme 4. The multi-step synthesis of dimer impurity or compound **19**.

near 3444, 1721, and 1652 cm^{-1} indicated the presence of NH (amidic), C=O (ketone) and C=O (amide) groups in compound **9**. The presence of OCH_3 and NH group was further supported by the ^{1}H signals at δ 4.06 (s, 3H) and 10.37 (bs, 1H) in the ^{1}H NMR spectra whereas the ^{13}C signals for C=O groups appeared in the region 175–161 ppm in the ^{13}C NMR spectra (Fig. 3). Notably, some of the ^{13}C signals were found to be splitted due to the C-F interactions.

The synthesis of other impurity i.e. compound **14** was carried out according to a multi-step method as presented in Scheme 3. The process involved acid catalyzed protection of the keto group of methyl-4-mehoxy acetoacetate (**10**) using ethylene glycol to give the ketal derivative **11** ester group of which was hydrolyzed in the presence of aqueous NaOH and catalytic Bu_4NBr in toluene to afford the desired acid derivative **12**. On treatment with $SOCl_2$ and catalytic DMF in toluene the acid **12** furnished the corresponding acid chloride *in situ* that on subsequent reaction with the 2,4-difluorobenzylamine in the presence of Et_3N in toluene gave the desired amide derivative **13**. The deprotection of the protected keto group of **13** afforded the desired compound **14** in 65% yield (with the HPLC purity of 97.45%). All the steps were carried out in the range of 7–10 g scale with minimum being 7 g for the 3rd step. The compound **14** was characterized with the help of IR, NMR and MS as well as HRMS data. The IR absorption at 3349 and 1659 cm^{-1} was due to the –NH(C=O)- moiety whereas that at 1731 cm^{-1} was due to the keto group. The presence of OCH_3 and NH group was further supported by the ^{1}H signals at δ 3.41 (s, 3H) and 7.18 (bs, 1H) in the ^{1}H NMR spectra whereas the ^{13}C signals for ketone and amide C=O group appeared at 203.8 and 165.2 ppm in the ^{13}C NMR spectra (Fig. 4). The ^{13}C signal at 59.2 ppm also confirmed the presence of OCH_3 group whereas the presence of three different type of methylene groups could be detected in both ^{1}H and ^{13}C NMR spectra of **14**. The splitting of ^{13}C signals to the C-F interactions were also observed in case of compound **14**.

The synthesis of compound **19** was carried out *via* another multi-step method (Scheme 4) similar to that of compound **14**. The ethyl 4-chloro acetoacetate was used as the starting compound in this case that on treatment with NaOEt in toluene afforded the ether derivative **15**. The acid catalyzed protection of the keto group of **15** using ethylene glycol gave a mixture of two ketal derivatives (**16**) one of which was generated due to the exchange of OEt group with ethylene glycol. However, the ester hydrolysis of the mixture of esters (**16**) afforded a single acid **17** that was converted to the corresponding acid chloride *in situ* and subsequently to the amide derivative **18** *via* the reaction with the 2,4-difluorobenzylamine. Notably, the deprotection of the protected keto group of **18** for a longer duration afforded the compound **19** in 75% yield (with the HPLC purity of 95.88%) rather than the corresponding deprotected ketone that seemed to be the intermediate in this transformation (Scheme 5). Thus a plausible reaction mechanism could be proposed for the formation of compound **19** that proceeded *via* the

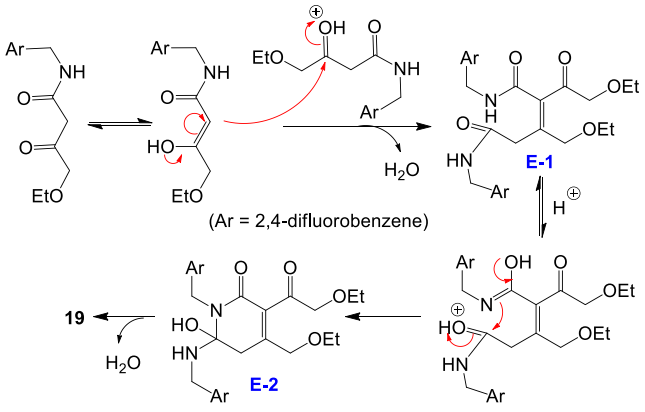

Scheme 5. The proposed reaction mechanism for the formation of compound **19**.

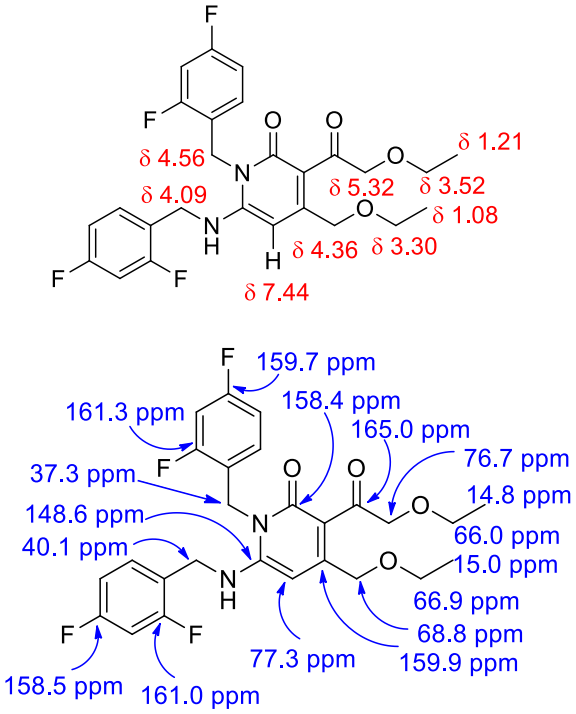

Fig. 5. Presentation of partial ^{1}H (red) and ^{13}C NMR data (blue) of compound **19**.

intermolecular reaction of deprotected ketone with another of its molecule to give the intermediate **E-1** followed by intramolecular cyclization and subsequent dehydration leading to the compound **19** *via* **E-2**.

In addition to the MS [*m/z*: 507 $(M+H)^+$] and HRMS [calcd for $C_{26}H_{26}F_4N_2O_4$ (M+H)+ 507.1862, found 507.1860] the NMR and IR spectra were analyzed for the characterization of compound **19** (Fig 5). The presence of four side chains was indicated by the ^{13}C signals at 14.8 (Me), 15.0 (Me), 37.3 (-CH_2N-), 40.1 (-CH_2NH-), 66.0 (-CH_2O-), 66.9 (-CH_2O-), 68.8 (-CH_2O-) and 76.7 (-COCH$_2$O-) ppm in the ^{13}CNMR spectra and was further supported by the ^{1}H signals at δ 1.08 (t, J = 6.8, 3H, CH_3), 1.21 (t, J = 6.8, 3H, CH_3), 3.30 (dd, J_1 = 6.8, J_2 = 7.2, 2H, OCH_2), 3.52 (dd, J_1 = 6.8, J_2 = 6.8, 2H, OCH_2), 4.09 (d, J = 12.0, 2H, CH$_2$NH),4.36 (s, 2H, OCH_2), 4.56 (d, J = 5.6, 2H, CH_2N), and 5.32 (s, 2H, $COCH_2O$) in the ^{1}HNMR spectra. The ^{13}C signal for C-5 of the central pyridinone ring appeared at 77.3 ppm in the ^{13}CNMR spectra whereas ^{1}H signal for the proton attached to the same carbon appeared at δ 7.44 in the ^{1}HNMR spectra.

Due to the reported interaction of dolutegravir with SARS CoV-2 OMTase *in silico* the selected synthesized compounds e.g. **7, 8** and **9** (structurally similar to dolutegravir) were docked into this protein. The docking studies of these compounds were carried out using the targeted protein e.g. SARS CoV-2 OMTase (PDB: 3R24). A graphical automatic drug design software i.e. the iGEMDOCK version2.1 (suitable for the docking, screening and analysis) [18,19] was employed for this study and outcomes are presented in Table 1. The estimated total energy suggested that the interaction of compound **7** with the protein was comparable or marginally better than that of dolutegravir whereas compounds **8** and **9** appeared to be relatively less effective.

To understand the observed behavior of compound **7** towards SARS CoV-2 OMTase its interactions with this protein along with compound **8** and **9** were analyzed and compared. When docked into SARS CoV-2 OMTase the molecule **7** (Fig. 6) formed H-bonds with TYR132 and CYS115 residues through its carbonyl group of the fused pyrazine and amidic NH moiety, π-π T shaped inter-

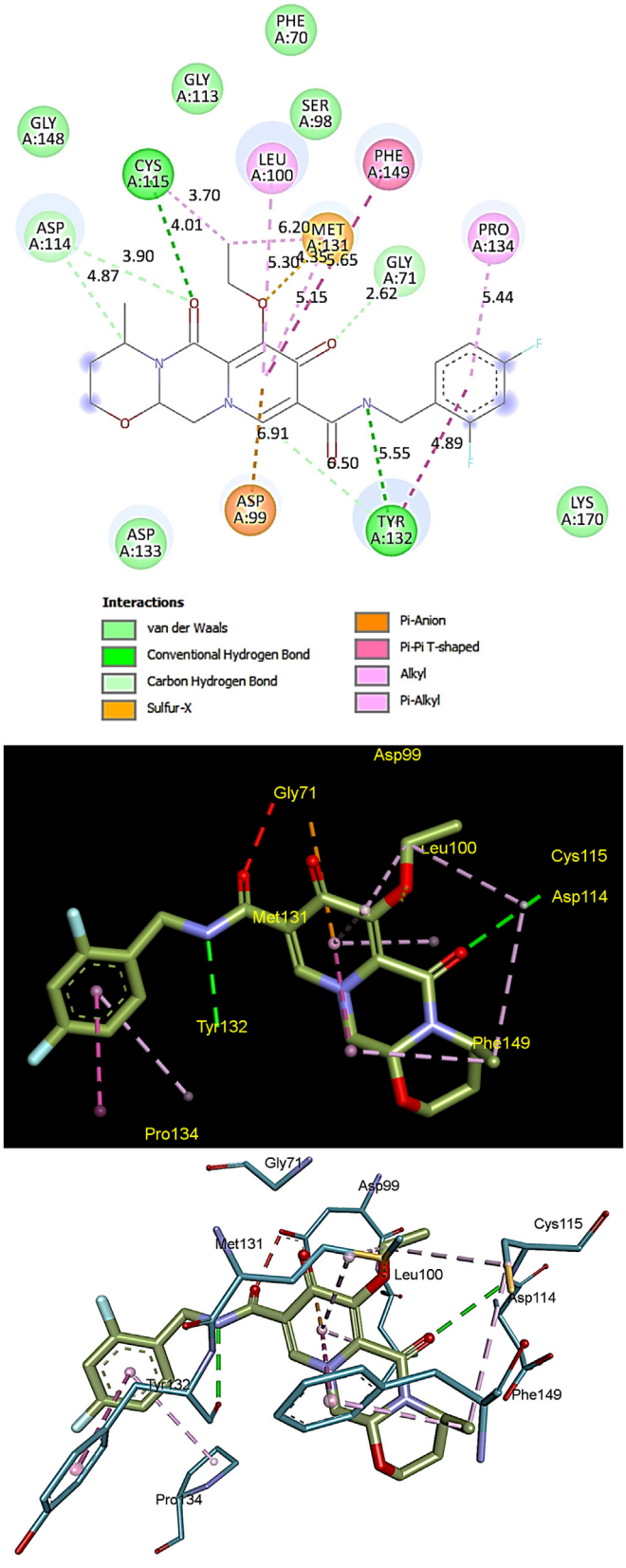

Fig. 6. The 2D and 3D interaction diagram of molecule **7** with SARS CoV-2 OMTase (PDB: 3R24).

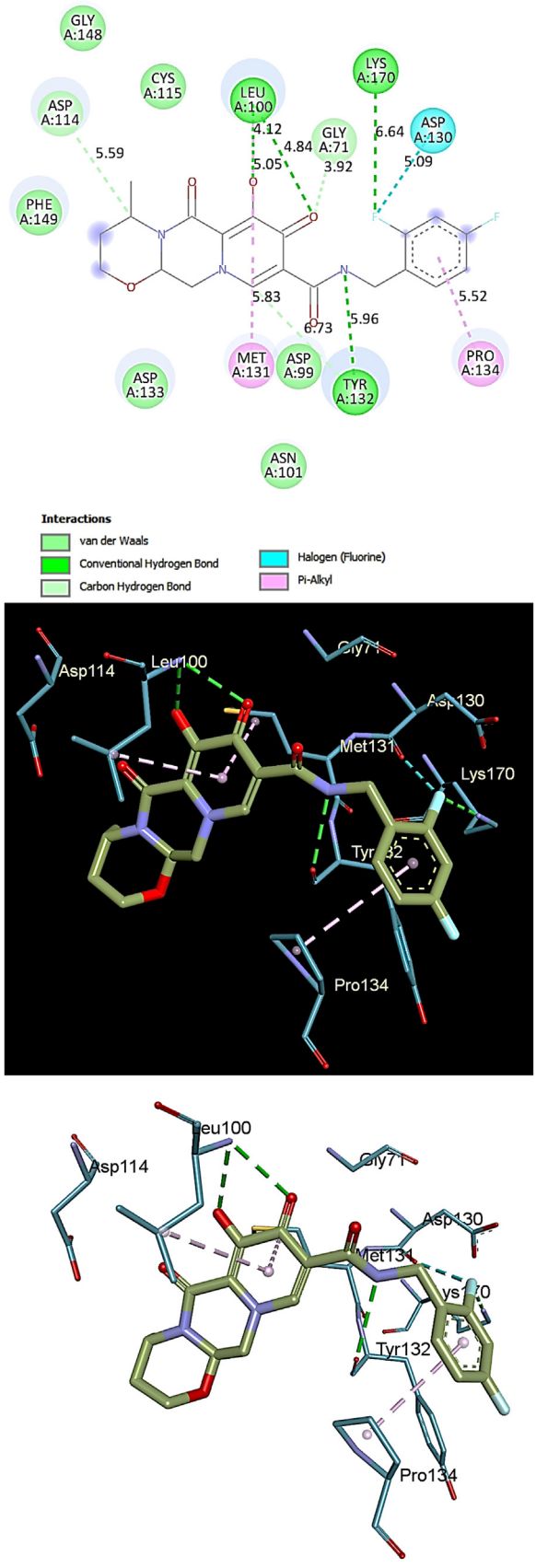

Fig. 7. The 2D and 3D interaction diagram of dolutegravir with SARS CoV-2 OMTase (PDB: 3R24).

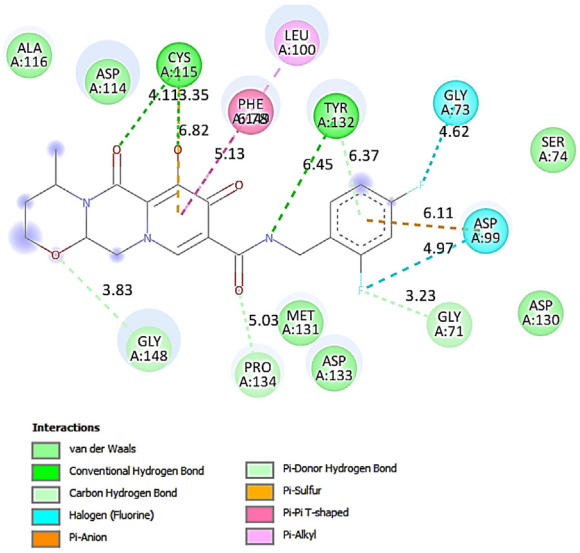

Fig. 8. The 2D interaction diagram of compound **8** with SARS CoV-2 OMTase (PDB: 3R24).

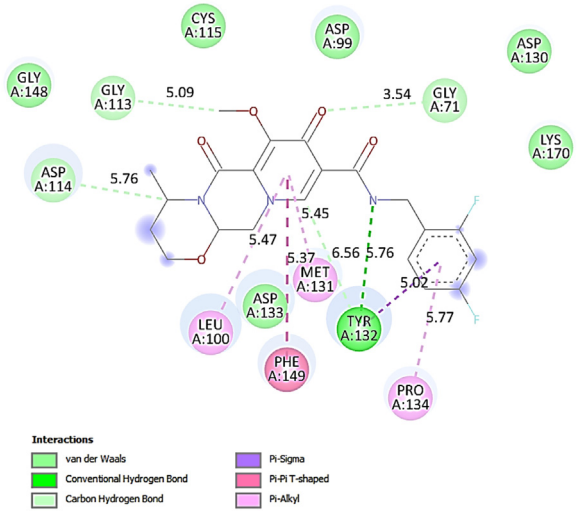

Fig. 9. The 2D interaction diagram of compound **9** with SARS CoV-2 OMTase (PDB: 3R24).

actions with PHE149 and TYR132 through its fused pyridine and 2,4-difluorobene rings. Besides, the molecule also participated in several other type of interactions such as van der Waals, π-alkyl, π-anion etc with the residues ASP99, PRO139, LEU100, ASP114, GLY71 and MET131. Particularly, the OEt side chain participated in alkyl and π-alkyl interactions that contributed significantly towards its overall interactions with the target protein. On the other hand, dolutegravir though formed H-bonds with TYR132, LYS170 and LEU100 (Fig. 7) its participation in other type of interactions with residues were rather lower in number. Like dolutegravir the compound **8** too had a free OH group but participated in lower number of H-bond interactions (Fig. 8) whereas in case compound **9** (Fig. 9) the presence of OMe group was not so favorable for strong interactions with SARS CoV-2 OMTase. Overall, besides its importance as one of the impurities of the marketed drug dolutegravir the compound **7** could be of interest as a possible inhibitor of SARS CoV-2 OMTase and may require *in vitro* / *in vivo* evaluations.

Table 1
Summary of interactions of compounds **7, 8, 9** and dolutegravir with SARS CoV-2 OMTase *in silico*.[a].

Compound	Estimated Total Energy (kcal/mol)	Active site interacting residues
7	-118.06	TYR132, CYS115, ASP99, PHE149, PRO139, LEU100, ASP114, GLY71, MET13111
8	-114.29	TYR132, CYS115, PRO134, GLY148, PHE149, LEU100, ASP99, GLY71, GLY73
9	-112.31	TYR132, PRO134, PHE149, LEU100, MET131, GLY71, ASP114, GLY113
Dolutegravir	-117.62	TYR132, LYS170, LEU100, MET131, ASP114, PRO134, ASP130, GLY71

[a] Residues involved in H-bonding are highlighted in blue color.

3. Conclusions

In conclusion, the synthesis and characterization of three impurities of dolutegravir including a new impurity were carried out successfully. The synthesis of O-methyl ent-dolutegravir was accomplished in three-steps the first one involved the construction of fused 1,3-oxazinane ring. The cleavage of –OEt ether moiety followed by methylation afforded the target compound that was characterized by the spectral data as well as HPLC and HRMS analysis. The second impurity i.e *N*-(2,4-difluorobenzyl)-4-methoxy-3-oxobutanamide was synthesized *via* a multi-step method involving sequentially the keto group protection, ester hydrolysis, acid chloride formation followed by the reaction with amine and finally keto group deprotection. The synthesis of third or new impurity was carried out *via* another multi-step method similar to the previous one starting from ethyl 4-chloroacetoacetate. The methodology involved preparation of ether derivative, keto group protection, ester hydrolysis, preparation of amide derivative *via* acid chloride formation *in situ* and then keto group deprotection for a longer duration. The last step afforded the target compound presumably *via* a self-condensation reaction of the deprotected keto compound generated *in situ* because of prolonged exposure to the acidic conditions. A plausible reaction mechanism has been proposed for this interesting transformation and the spectral characterization of the isolated product is presented. All three impurities were prepared in gram scale (minimum 2 g and maximum 8 g) indicating suitability and potential of theses developed methodologies for the laboratory as well as large scale preparations. Moreover, as reference standards the synthesized compounds might be useful for R&D centers and organizations involved in API research and bulk drug manufacturing. The *in silico* evaluation of three selected synthesized intermediates e.g. **7, 8** and **9** (structurally similar to dolutegravir) against SARS CoV-2 OMTase (PDB: 3R24) indicated that compound **7** could be of interest as a possible inhibitor of this protein and may require *in vitro* | *in vivo* studies. Collectively, the current study would be of interest not only from the view point of process development for producing and profiling chemically pure dolutegravir but also in the context of COVID-19.

4. Experimental section

4.1. General information

The main suppliers of all chemicals (reagent grade) were Spectrochem, Alfa Aesar (India) and TCI. The silica gel 60 GF254 sheets (E. Merck, Germany) were used to run TLC (thin layer chromatography) and visualization was done using the UV light (254 nm). Normal-phase HPLC analysis was carried out using Hypersil BDS C18 150 mm x 4.6 × 3 µ. A Perkin-Elmer BX series FT-IR spectrometer was used for recording the IR spectra (KBr pellet). ^{1}H & ^{13}C NMR spectra were recorded using a ^{1}H-Varian-Mercury-400 spectrometer. Chemical shift values are given in ppm (δ) using TMS as internal standard. A Mariner System 5304 MS spectrometer was used to record the ESI MS. The Q-TOF Micro mass spectrometer was used for recording the HRMS (high resolution mass spectra).

4.2. HPLC method

4.2.1. Mobile phases preparation

The mobile phases were prepared as follows: Mobile Phase A: 0.5 mM of EDTA disodium solution was prepared by dissolving 186 mg of EDTA disodium dihydrate in 1000 mL of Millipore water (degassed by ultrasonic method). Mobile Phase B: 1.0 mL of TFA was taken into 1000 mL of acetonitrile and mixed well. Diluent (Blank): A mixture of water and acetonitrile in the ratio of 8:2 (v/v) was employed.

4.2.2. Solution preparation: impurity stock solution

12.5 mg of each impurity was weighed and transferred into a 50 mL volumetric flask and to it, 30 mL of diluent was added and sonicated to dissolve the impurity. Then the diluent was added up to the mark and mixed well. **System suitability solution:** in a volumetric flask (50 mL) was taken the dolutegravir standard (25 mg) to which was added the diluent (30 mL) and impurity stock solution (1 mL). Then sonication was used to result complete dissolution and the solution was diluted up to the mark with diluent and mixed well. **Sample Solution:** 25.0 mg of the sample was weighed and transferred into 50 mL of brown volumetric flask. The diluent (30 mL) was added and sonicated to result complete dissolution. The resulting solution was diluted to the mark with diluent and mixed well. **The employed column parameters:** Column: Hypersil BDS C18 150 mm x 4.6 × 3 µ; Column temperature: 35 °C; Detector: UV; Wavelength: 258 nm; Flow rate: 1.0 mL/min; Injection volume: 10 µL; Running time: 50 min; Data Acquisition time: 40 min. Needle washing solution: acetonitrile: water = 1: 1 or acetonitrile.

4.3. Preparation of (4S,12aR)-N-(2,4-difluorobenzyl)-7-ethoxy-4-methyl-6,8-dioxo-3,4,6,8,12,12a-hexahydro-2H-pyrido[1′,2′:4,5]pyrazino[2,1-b][1,3]oxazine-9-carboxamide (7)

To a solution of compound **1** (5 g, 12 mmol) in toluene (25 mL, 5 vol) was added methanol (1.1 g, 35 mmol) and acetic acid (1.6 g, 26 mmol). To this was added compound **6** (1.3 g, 14 mmol) in toluene (25 mL, 5 vol) at room temperature and then the temperature of the reaction mass was raised to 95 °C. The temperature was maintained for 5 h. After completion of the reaction (indicated by TLC), the reaction mass was cooled to room temperature and diluted with cold water (50 mL, 10 vol). The separated organic layer was collected and the aqueous layer was repeatedly extracted with toluene (50 mL, 2 × 5 vol). All the organic layers were combined, washed with saturated sodium bicarbonate solution (25 mL, 5 vol) followed by cold water (25 mL, 5 vol) and concentrated under vacuum at 50 °C to give the crude compound. The compound was then washed with methyl isobutyl ketone (or MIBK, 15 mL, 3 vol) and dried under vacuum at 40 °C for 3 h. The title compound was isolated as a pale yellow solid in 80% yield (4.2 g); ^{1}H NMR (400 MHz, $CDCl_3$): δ 1.35 (d, J = 7.2 Hz, 3H), 1.47 (t, J = 7.0 Hz,

3H), 1.53 (d, J = 1.6 Hz, 1H), 2.15- 2.20 (m, 1H), 3.96 (t, J = 9.2 Hz, 2H), 4.11 (dd, J_1 = 6.0 Hz, J_2 = 7.2 Hz, 1H), 4.22–4.27 (m, 3H), 4.61 (d, J = 6.0 Hz, 2H), 5.01 (t, J = 6.0 Hz, 1H), 5.18–5.20 (m, 1H), 6.79–6.83 (m, 2H), 7.3–7.38 (m, 1H), 8.36 (s, 1H), 10.36 (d, J = 4.8 Hz, 1H); Mass *m/z*: 448 $(M+H)^+$.

*4.4. Preparation of (4S,12a*R*)-N-(2,4-difluorobenzyl)-7-hydroxy-4-methyl-6,8-dioxo-3,4,6,8,12,12a-hexahydro-2*H*-pyrido[1′,2′:4,5]pyrazino[2,1-*b*][1,3]oxazine-9- carboxamide (8)*

A solution of sodium ethoxide (3.4 g, 85 mmol) in ethanol (25 mL, 5 vol) was stirred for 30 min at room temperature. The reaction mass was cooled to 10 °C and a solution of compound **7** (5 g, 11 mmol) dissolved in DCM (15 mL, 3 vol) was added. The temperature of the reaction mass was raised to room temperature and maintained for 12 h. After completion of the reaction (indicated by TLC), the reaction mass was cooled to 10 °C and diluted with water (25 mL, 5 vol) followed by DCM (25 mL, 5 vol). Then 6 N HCl was added to the reaction mass until the pH of the solution reached to 1–2. The separated organic layer was collected and the aqueous layer was repeatedly extracted with DCM (50 mL, 2 × 5 vol). The combined organic layer was washed with saturated sodium bicarbonate solution (50 mL, 2 × 5 vol), followed by distilled water (25 mL, 5 vol) and concentrated under vacuum at 35 °C to give the crude compound. The crude was washed with ethanol (10 mL, 2 vol) and dried under vacuum at 40 °C to give the compound **8** as a light brown solid in 70% yield (3.3 g); HPLC purity: 99.03%; mp:174.2–175.4 °C; ^{1}H NMR (400 MHz, DMSO-d_6): δ 1.33 (d, J = 6.8 Hz, 3H), 1.54 (d, J = 13.2 Hz, 1H), 1.98–2.05 (m, 1H), 3.89 (dd, J_1 = 3.2 Hz, J_2 = 3.2 Hz, 1H), 4.03 (t, J = 11.2 Hz, 1H), 4.35 (dd, J_1 = 6.0 Hz, J_2 = 5.6 Hz, 1H), 4.56 (dd, J_1 = 5.2 Hz, J_2 = 4.0 Hz, 3H), 4.79 (t, J = 6.4 Hz, 1H), 5.45 (t, J = 4.8 Hz, 1H) 7.03–7.08 (m, 1H), 7.21–7.26 (m, 1H), 7.36–7.40 (m, 1H), 8.49 (s, 1H), 10.36 (t, J = 5.6 Hz, 1H), 12.50 (bs, 1H); Mass *m/z*: 420 $(M+H)^+$.

*4.5. Preparation of (4S,12a*R*)-*N*-(2,4-difluorobenzyl)-7-methoxy-4-methyl-6,8-dioxo-3,4,6,8,12,12a-hexahydro-2*H*-pyrido[1′,2′:4,5]pyrazino[2,1-*b*][1,3]oxazine-9-carboxamide (9)*

To a solution of compound **8** (2.5 g, 60 mmol) in acetone (25 mL, 10 vol) was added K_2CO_3 (1.2 g, 87 mmol) at room temperature. Then dimethyl sulfate (0.9 g, 72 mmol) was added to the reaction mass at room temperature and the same temperature was maintained for 3 h. After completion of the reaction, the reaction mass was filtered and the cake was washed with acetone (5 mL, 2 vol). The filtrates were collected, combined, and concentrated under vacuum at 45 °C, The residue· obtained was dissolved in DCM (12.5 mL, 5 vol) and washed with water (7.5 mL, 3 vol). The DCM layer was collected, dried over anhydrous sodium sulfate, filtered and concentrated under vacuum at 40 °C to give the compound **9** as a viscous liquid in 80% (2.1 g) yield; HPLC purity: 95.66%; IR (cm^{-1}): 3444, 2933, 2248, 1721, 1651, 1505, 1549, 1429, 1352, 1274; HPLC purity: 95.66%; IR (cm^{-1}): 3444, 2933, 2248, 1721, 1651, 1505, 1549, 1429, 1352, 1274; ^{1}H NMR (400 MHz, $CDCl_3$): δ 1.32 (d, J = 6.8 Hz, 3H), 1.45 (d, J = 13.6 Hz, 1H), 2.09–2.15 (m, 1H), 3.67 (s, 1H), 3.93 (s, 1H), 4.06 (s, 3H), 4.09 (d, J = 4.8 Hz, 1H), 4.24 (d, J = 11.6 Hz, 1H), 4.54 (d, J = 4.4 Hz, 2H), 4.92 (t, J = 6 Hz, 1H), 5.13 (s, 1H), 6.71 (t, J = 8.4 Hz, 1H), 7.20–7.27 (m, 1H), 7.94 -8.11 (m, 1H), 8.41 (s, 1H), 10.37 (s, 1H, NH): ^{13}C NMR (100 MHz, $CDCl_3$): δ 15.5 (Me), 29.6 (-CH_2NH-), 36.6 (CH_2), 44.7 (-CHMe-), 52.3 (OMe), 61.1 (NCH_2-), 62.5 (–OCH_2-), 76.1 (-OCH-), 103.7, 111.3, 118.6, 121.3, 130.5, 136.1, 142.4, 155.6, 155.9, 161.9 (dd, J = 249 & 12 Hz), 162.4, 163.4, 164.2, 174.5 (C=O); Mass *m/z*: 434 $(M+H)^+$; HRMS (ESI –MS) calcd for $C_{21}H_{21}F_2N_3O_5$ (M+H)+ 434.1483, found 434.1481.

4.6. Preparation of methyl 2-(2-(methoxymethyl)-1,3-dioxolan-2-yl)acetate (11)

To solution of *p*-toluene sulphonic acid mono hydrate (1.3 g, 6 mmol) and ethylene glycol (10 mL, 1 vol), methyl-4-mehoxy acetoacetate **10** (10 g, 68 mmol) in toluene (150 mL, 15 vol) was added at room temperature. The reaction temperature was raised to azotropic reflux 110–115 °C for 3 h. After completion of the reaction, the reaction mass was cooled to room temperature. The toluene and ethylene glycol layers were separated. The ethylene glycol layer was collected and extracted repeatedly with DCM (3 × 2 vol). The DCM extracts were collected, combined, concentrated under vacuum at 55–60 °C to give the compound **11** as a brown color liquid in 100% (13.2 g) yield; ^{1}HNMR (400 MHz, $CDCl_3$) δ 2.79 (s, 2H), 3.41 (s, 3H), 3.50 (s, 2H), 3.69 (s, 3H), 4.01–4.02 (m, 4H); Mass *m/z*: 191 $(M+H)^+$.

4.7. Preparation of 2-(2-(methoxymethyl)-1,3-dioxolan-2-yl)acetic acid (12)

To a solution of NaOH (8.2 g, 20 mmol) in water (65 mL) was added tetra butyl ammonium bromide (0.22 g, 6 mmol) and compound **11** (13.0 g, 68 mmol) in toluene (65 mL, 5 vol). The reaction mass was stirred at room temperature for 10 min and then the temperature was raised to 40 °C for 3 h. After completion of the reaction, the reaction mass was cooled to room temperature. The separated aqueous layer was extracted repeatedly using 10% methanol in DCM (2 × 2.5 vol). The aqueous layer was collected, cooled to 0 °C, the pH was adjusted to 1 using 6 N HCl and was extracted repeatedly using DCM (3 × 5 vol). The organic extracts were collected, combined, dried over anhydrous sodium sulfate, filtered and concentrated at 35 °C under vacuum to give the compound **12** as an oily liquid in 60% (7.2 g) yield; ^{1}HNMR (400 MHz, $CDCl_3$) δ 2.82 (s, 2H), 3.42 (s, 3H), 3.51 (s, 2H), 4.00–4.08 (m, 4H): Mass *m/z*: 177 $(M+H)^+$

4.8. Preparation of N*-(2,4-difluorobenzyl)-2-(2-(methoxymethyl)-1,3-dioxolan-2-yl)acetamide (13)*

A solution of compound **12** (7 g, 39 mmol) in toluene (35 mL, 5 vol) and DMF (0.3 mL, 0.05 vol) was cooled to 0 °C. To this was added thionyl chloride (5.2 g, 43 mmol) at 0 °C. The reaction temperature was then raised to room temperature and left it for 2 h. In another vessel a solution of 2,4-difluoro benzylamine (6.2 g, 43 mmol) in toluene (35 mL, 5 vol) was taken at room temperature to which was added triethylamine (10.0 g, 99 mmol). The mixture was then cooled to 0 °C to which was added the above mentioned acid chloride solution at 0 °C. The temperature was then raised to room temperature and left for 3 h. After completion of the reaction, distilled water (70 mL, 10 vol) was added to the reaction mass. The separated aqueous layer was extracted with toluene (70 mL, 10 vol). The organic extracts were collected, combined, washed with 2 N HCl (35 mL, 5 vol) followed by saturated $NaHCO_3$ solution (35 mL, 5 vol) and distilled water (35 mL, 5 vol). The organic layer was concentrated under vacuum at 60 °C to give the compound **13** as a thick viscous liquid in 76% (9.1 g) yield; ^{1}HNMR (400 MHz, $CDCl_3$) δ 2.68 (s, 2H) 3.35 (s, 5H), 3.90–4.0 (m, 4H), 4.43 (d, J = 6.0, 2H), 6.62 (bs, 1H), 6.77–6.86 (m, 2H), 7.34–7.40 (m, 1H): Mass *m/z*: 302 $(M+H)^+$

4.9. Preparation of N-(2,4-difluorobenzyl)-4-methoxy-3-oxobutanamide(14)

To a solution of compound **13** (9 g, 43 mmol) in toluene (90 mL, 10 vol) was added 2 N HCl (90 mL, 10 vol) and tetrabutyl ammoniumbromide (0.1 g, 4 mmol) at room temperature. The temperature

was raised to 80–85 °C for 12 h. Then the mixture was cooled to room temperature. The separated aqueous layer was extracted with toluene (45 mL, 5 vol). The organic extracts were collected, combined, washed with saturated $NaHCO_3$ solution (45 mL, 5 vol), concentrated under vacuum at 60 °C to afford the crude product. To the crude product was added cyclohexane (45 mL, 5 vol) and the mixture was stirred for 30 min at 0 °C. After filtration the cake was washed with cyclohexane and dried under vacuum at 40–45 °C for 4 h to give the compound **14** as an off-white solid in 65% (4.8 g) yield: HPLC Purity: 97.45%: mp: 56.2–59.4 ºC; ^{1}HNMR (400 MHz, $CDCl_3$) δ 3.41 (s, 3H), 3.47 (s, 2H), 4.08 (s, 2H), 4.45 (d, J = 6.0, 2H), 6.77–6.86 (m, 2H) 7.18 (bs, 1H), 7.27–7.35 (m, 1H): ^{13}CNMR (100 MHz, $CDCl_3$) δ 36.9, 45.7, 59.2, 77.4, 104.0, 111.3, 120.8, 130.8, 159.6, 161.0 (dd, J = 249 & 12 Hz), 165.2, 203.8; IR (cm^{-1}) 3349, 3287, 3085, 2932, 1731, 1659, 1555, 1506; Mass *m/z*: 258 $(M+H)^+$; HRMS (ESI–MS) calcd for $C_{12}H_{13}F_2NO_3$ $(M+H)^+$ 258.0683, found 258.0682.

4.10. Preparation of ethyl 4-ethoxy-3-oxobutanoate (15)

A solution of NaOEt (18.6 g, 27 mmol) in toluene (60 mL, 4 vol) was cooled to 5–10 °C, and then ethyl-4-chloro acetoacetate **14** (15 g, 91 mmol) in toluene (60 mL,4 vol) was added. The reaction temperature was raised to 40 °C and maintained it for 3 h. After completion of the reaction, the reaction mass was cooled to 0 °C and the pH was adjusted to 1 using 2 N HCl. The seperated aqueous layer was extracted with toluene (5 vol). The organic extracts were collected, combined, washed with saturated $NaHCO_3$ solution (2 × 5 vol) followed by distilled water (5 vol). The organic layer was concentrated under vacuum at 55 °C to give the compound **15** as a brown liquid in 100 % (15.8 g) yield; ^{1}H NMR (400 MHz, $CDCl_3$) δ 1.24 (t, J = 6.8, 3H), 1.28 (t, J = 7.2, 3H), 3.52 (s, 2H), 3.53–3.58 (m, 2H), 4.02 (s, 2H), 4.11–4.22 (m, 2H); Mass *m/z*: 175 $(M+H)^+$.

4.11. Preparation of 2-hydroxyethyl 2-(2-(ethoxymethyl)-1,3-dioxolan-2-yl)acetate (16)

To a mixture of *p*-toluenesulphonic acid mono hydrate (1.7 g, 9 mmol) and ethylene glycol (15 mL, 1 vol) in toluene (150 mL, 10 vol) was added the compound **15** (15 g, 10 mmol) at 25 °C. The temperature was then raised to the azotropic reflux temperature i.e. 110–115 ºC and maintained for 3 h. Then, the reaction mixture was cooled to 25 °C. The separated ethylene glycol layer was extracted with dichloromethane (3 × 2 vol). The organic extracts were collected, combined, concentrated under vacuum at 60 °C to give the compound **15** as a brown color liquid in 67% (13.2 g) yield; mass *m/z* = 219 $(M+H)^+$. This product was taken forward directly to the next step.

4.12. Preparation of 2-(2-(ethoxymethyl)-1,3-dioxolan-2-yl)acetic acid (17)

To a solution of sodium hydroxide (7.2 g, 18 mmol) in water (65 mL, 5 vol) was added tetrabutyl ammonium bromide (0.2 g, 6 mmol) and compound **16** (13.0 g, 59 mmol) in toluene (65 mL, 5 vol) at 25 °C and the mixture was stirred for 10 min. The reaction temperature was raised to 40 °C for 3 h. Then the mixture was cooled to room temperature. The separated aqueous layer was extracted using 10% methanol in dichloromethane (2 × 2.5 vol). The aqueous layer was collected, cooled to 0 °C and the pH was adjusted to 1 using 6 N HCl (39 mL, 3 vol). The extraction of aqueous layer was carried out using DCM (3 × 5 vol). The organic extracts were collected, combined, dried over anhydrous sodium sulfate, filtered and concentrated at 35 °C under vacuum to give the compound **17** as an oily liquid in 64% (7.2 g) yield; ^{1}H NMR (400 MHz, $CDCl_3$) δ 1.21 (t, J = 6.8, 3H), 2.8 (s, 2H), 3.54 (s, 2H), 3.56–3.61 (m, 2H), 4.01–4.05 (m, 4H); Mass *m/z*: 191$(M+H)^+$

4.13. Preparation of N-(2,4-difluorobenzyl)-2-(2-(ethoxymethyl)-1,3-dioxolan-2-yl)acetamide (18)

A solution of compound **17** (7 g, 36 mmol) in toluene (35 mL, 5 vol) and DMF (0.05 eq) was cooled to 0 °C and thionyl chloride (4.8 g, 40 mmol) was added, then the temperature was raised to 25 °C and maintained for 2 h. In a separate vessel the 2,4-difluoro benzylamine (5.8 g, 40 mmol) in toluene (35 mL, 5 vol) and triethylamine (9.3 g,9 mmol) was taken at 25 °C and the solution was cooled to 0 °C. To this was added the above mentioned acid chloride solution at 0 °C and the temperature was raised to 25 °C that was maintained for 3 h. After completion of the reaction, distilled water (70 mL, 10 vol) was added to the reaction mass. The separated aqueous layer was extracted with toluene (70 mL, 10 vol). The organic layers were collected, combined, washed with 2 N HCl (35 mL, 5 vol) followed by saturated $NaHCO_3$ solution (35 mL, 5 vol) and distilled water (35 mL, 5 vol), concentrated under vacuum at 60 °C to give the compound **18** as a thick viscous liquid 77 % (9 g) yield; ^{1}H NMR (400 MHz, $CDCl_3$) δ 1.16 (t, J = 6.8, 3H), 2.69 (s, 2H), 3.39 (s, 2H), 3.47–3.53 (m, 2H), 3.89–4.01 (m, 4H), 4.43 (d, J = 6.0, 2H), 6.68 (bs, 1H), 6.67–6.86 (m, 2H), 7.34–7.39 (m, 1H); Mass *m/z*: 316 $(M+H)^+$.

4.14. Preparation of 1-(2,4-difluorobenzyl)-6-((2,4-difluorobenzyl)amino)-3-(2-ethoxyacetyl)-4-(ethoxymethyl)pyridin-2(1H)-one (19)

A solution of compound **18** (7 g, 22 mmol) in toluene (70 mL, 10 vol), 6 N HCl (70 mL, 10 vol) and tetrabutyl ammonium bromide (0.07 g, 2 mmol) was heated to 80–85 °C for 24 h. Then the mixture was cooled to 25 °C. The separated aqueous layer was extracted with toluene (45 mL, 5 vol). The organic layers were collected, combined, washed with saturated $NaHCO_3$ solution (45 mL, 5 vol), concentrated under vacuum at 60 °C to give the compound **19** as a dark brown solid in 75% (8.4 g) yield: HPLC Purity:-95.88%: mp: 115.2–118.6 °C; ^{1}H NMR (400 MHz, DMSO-d_6) δ 1.08 (t, J = 6.8, 3H), 1.21 (t, J = 6.8, 3H), 3.30 (dd, J_1 = 6.8, J_2 = 7.2, 2H), 3.52 (dd, J_1= 6.8, J_2 = 6.8, 2H), 4.09 (d, J = 12.0, 2H), 4.36 (s, 2H), 4.56 (d, J = 5.6, 2H), 5.32 (s, 2H), 6.73–7.02 (m, 6H), 7.27 (s, 1H), 7.41–7.47 (m, H); ^{13}CNMR (100 MHz, DMSO-d_6) 14.8, 15.0, 37.3, 40.1, 66.0, 66.9, 68.8, 76.7, 77.3, 103.7, 104.2,114.4, 117.7, 111.9, 128.9, 129.0, 131.7, 131.8, 148.6, 158.4, 158.5, 159.7, 159.9, 161.0, 161.3 (dd, J = 249 & 12 Hz), 165.0; IR (cm^{-1}) 3253, 3073, 2975, 2878, 1661, 1619, 1543, 1504, 1428, 1277; Mass *m/z* 507 $(M+H)^+$; HRMS (ESI –MS) calcd for $C_{26}H_{26}F_4N_2O_4$ $(M+H)+$ 507.1862, found 507.1860.

4.15. Docking studies

The docking studies for the assessment of binding mode and interactions of the test molecules were carried out using the iGEMDOCK version2.1 software (http://gemdock.life.nctu.edu.tw/dock/). This is a graphical –automatic drug design system generally used for docking, screening and analysis. The *in silico* docking simulation studies were performed to evaluate the molecular interactions of test compounds and dolutegravir with the SARS CoV-2 OMT (PDB: 3R24) protein with a co-crystallized ligand (SAM). The 2D structure of the ligands was drawn through BIOVIA Draw software and saved in mol format. The Avogadro software was used to optimize and minimize the ligand structures. The macromolecules were cleaned from water residues and Gasteiger charges were added through Dock Prep in UCF Chimera. The Discovery Visualizer (Biovia) was used to visualize and analyze the Ligand interactions. Standard

docking protocol was followed and stable docking method was selected. Based on the scoring function the best docking solutions were analyzed. The scoring function estimates the fitness by combining van der Waals, H-bonding and electro statistic energies. Post docking interaction profile analysis of best poses was conducted to determine the interactions between the ligand and the target protein.

Declaration of Competing Interest

The authors declare that they have no known competing financial interests or personal relationships that could have appeared to influence the work reported in this paper.

CRediT authorship contribution statement

Sailaja Garrepalli: Conceptualization, Validation, Methodology, Writing – original draft. **Ramesh Gudipati:** Conceptualization, Validation, Methodology, Writing – original draft. **Ravikumar Kapavarapu:** Methodology. **Kunta Ravindhranath:** Conceptualization, Supervision. **Manojit Pal:** Conceptualization, Supervision.

Data Availability

All the data are included either in the manuscript or in the supporting information.

Acknowledgement

We thank the management of Koneru Lakshmaiah Education Foundation, Vaddeswaram, Andhra Pradesh, India and Synix Labs, Hyderabad, India for encouragement and support.

Supplementary materials

Supplementary material associated with this article can be found, in the online version, at doi:10.1016/j.molstruc.2022.133992.

References

[1] M. Vitoria, A.M. Hill, N.P. Ford, M. Doherty, S.H. Khoo, A.L. Pozniak, Choice of antiretroviral drugs for continued treatment scale-up in a public health approach: What more do we need to know? J. Int. AIDS Soc. 19 (2016) 20504–20512.

[2] J. Gallant, J. Andrade-Villanueva, P. Chetchotisakd, E. DeJesus, F. Antunes, K. Arastah, Cobicistat versus ritonavir as a pharmacoenhancer of atazanavir plus emticitabine/tenofovir disoproxil fumarate in treatment-naive HIV type 1-infected patients: week 48 results, J. Infect. Dis. 20 (2013) 32–39.

[3] R. Cooper, N. Wiebe, N. Smith, P. Keiser, S. Naicker, M. Tonelli, Systematic review and meta-analysis: renal safety of tenofovir disoproxil fumarate in HIV-infected patients, Clin. Infect. Dis. 51 (2010) 496–505.

[4] S.G. Harjivan, C. Charneira, I.L. Martins, S.A. Pereira, G. Espadas, E. Sabidó, F.A. Beland, M.M. Marques, A.M.M. Antunes, Covalent histone modification by an electrophilic derivative of the anti-HIV drug nevirapine, Molecules 26 (2021) 1349.

[5] T. Abuduaini, V. Roy, J. Marlet, C. Gaudy-Graffin, D. Brand, C. Baronti, F. Touret, B. Coutard, T.R. McBrayer, R.F. Schinazi, L.A. Agrofoglio, Synthesis and antiviral evaluation of (1,4-Disubstituted-1,2,3-Triazol)-(*E*)-2-Methyl-but-2-Enyl nucleoside phosphonate prodrugs, Molecules 26 (2021) 1493, doi:10.3390/molecules26051493.

[6] A. Pendri, N.A. Meanwell, K.M. Peese, M.A. Walker, New first and second generation inhibitors of human immunodeficiency virus-1 integrase, Expert Opin. Ther. Pat. 21 (2011) 1173–1189.

[7] L. De Luca, S. De Grazia, S. Ferro, R. Gitto, F. Christ, Z. Debyser, A. Chimirri, HIV-1 integrase strand-transfer inhibitors: design, synthesis and molecular modeling investigation, Eur. J. Med. Chem. 46 (2011) 756–764.

[8] R.J. Khan, R.K. Jha, G.M. Amera, M. Jain, E. Singh, A. Pathak, R.P. Singh, J. Muthukumaran, A.K. Singh, Targeting SARS-CoV-2: a systematic drug repurposing approach to identify promising inhibitors against 3C-like proteinase and 2′-O-ribose methyltransferase, J. Biomol. Struct. Dyn. 39 (2021) 2679–2692, doi:10.1080/07391102.2020.1753577.

[9] B.R. Beck, B. Shin, Y. Choi, S. Park, K. Kang, Predicting commercially available antiviral drugs that may act on the novel coronavirus (SARS-CoV-2) through a drug-target interaction deep learning model, Comput. Struct. Biotechnol. J. 18 (2020) 784–790.

[10] Therapieoptionen und klinische Studien zu neuartigem Coronavirus 2019-nCoV. 26.06.2020. URL: https://www.sciencemediacenter.de/alle-angebote/fact-sheet/details/news/therapieoptionen-bei-coronavirus-infektion/.

[11] B.A. Johns, T. Kawasuji, T. Taishi, Y. Taoda, Polycyclic carbamoylpyridone derivative having HIV integrase inhibitory activity. World Patent Application No WO2006/116764A1, 28 April 2006.

[12] C. Satyanarayana, G.S.R. Anjaneyulu, D.V.L. Narasimha, K.M. Bushan, A. Ravindra, Novel process for the preparation of dolutegravir and pharmaceutically acceptable salts thereof, World Patent Application No: WO 2015/110897 A2, 30 July 2015.

[13] S. Sankareswaran, M. Mannam, V. Chakka, S.R. Mandapati, P. Kumar, Identification and control of critical process impurities: an improved process for the preparation of dolutegravir sodium, Org. Process Res. Dev. 20 (2016) 1461–1468.

[14] M.R. Gudisela, P. Bommu, S. Navuluri, N. Mulakayala, Synthesis and characterization of potential impurities of dolutegravir: a HIV drug, ChemSelect 3 (2018) 7152–7155, doi:10.1002/slct.201800948.

[15] S. Garrepalli, R. Gudipati, S.R. Amasa, K. Ravindhranath, M. Pal, Synthesis of two diastereomeric impurities of a fluorinated antiretroviral drug dolutegravir, J. Mol. Struct. 1253 (2022) 132274, doi:10.1016/j.molstruc.2021.132274.

[16] J. Roy, Pharmaceutical impurities-a mini-review, AAPS PharmSciTech 3 (2002) 1–8, doi:10.1208/pt030206.

[17] P. Pojashree, T. Parmila, S.M. Kumar, G.P.S. Kumar, A review on pharmaceutical impurities and its importance in pharmacy, Am. J. PharmTech Res. 9 (2019) 76–87 http://ajptr.com/assets/upload/publish_article/AJPTR_95007.pdf.

[18] J.M. Yang, C.C. Chen, GEMDOCK: a generic evolutionary method for molecular docking, Proteins 55 (2004) 288–304, doi:10.1002/prot.20035.

[19] iGEMDOCK (2022) A graphical environment for recognizing pharmacological interactions and virtual screening, see: http://gemdock.life.nctu.edu.tw/dock/igemdock.php.